

## Chapter 4

### Selective Growth of GaAs by Shadow Mask Technique

#### 4.1 Preparation of Shadow Mask

The shadow mask consists of MBE grown  $\text{Ga}_{0.58}\text{Al}_{0.42}\text{As}$  and GaAs layers. After the (100) semi-insulator GaAs substrate was already prepared in the growth chamber, the  $\text{Al}_{0.58}\text{Ga}_{0.42}\text{As}$  layer, so-called *mask spacer* was grown for 3  $\mu\text{m}$  thick. The Al contents and layer thickness have been proved by using double crystal X-ray diffraction (DCXRD) rocking curve technique as shown in the figure 4.1.

The GaAs layer was then consecutively grown over the top surface of the mask spacer for about 1  $\mu\text{m}$  thick. This GaAs layer is called a *mask layer*. Figure 4.2 is a secondary electron microscopy image (SEM) from the cutting edge of the GaAs and  $\text{Al}_{0.58}\text{Ga}_{0.42}\text{As}$  epitaxial grown on the GaAs substrate. The interfaces are clear to see and indicated in the figure. The growth process of these two layers must be carefully controlled for mirror-like GaAs surface reward. The top surface of the mask layer is important to use as a dummy layer for the secondary MBE growth because of it is not possible to verify the selective growth surface under the shadow mask with RHEED. It is assumed that when the top surface of the mask layer is already oxide-desorbed, the opening substrate surface under the shadow mask should be also cleaned.

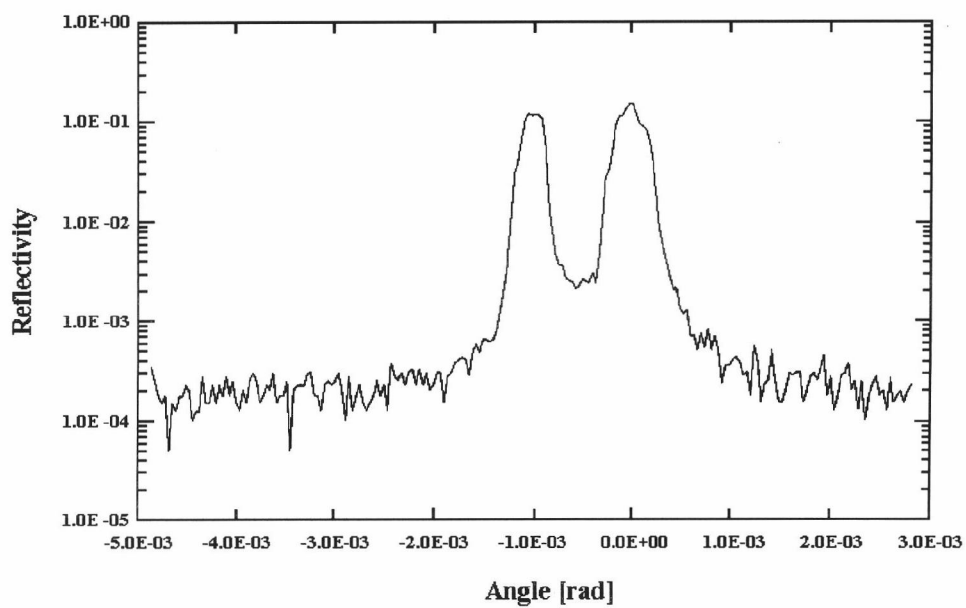


Figure 4.1 The DCXRD rocking curve pattern from the  $\text{Al}_{0.58}\text{Ga}_{0.42}\text{As}/\text{GaAs}$  epitaxial grown on the GaAs substrate.

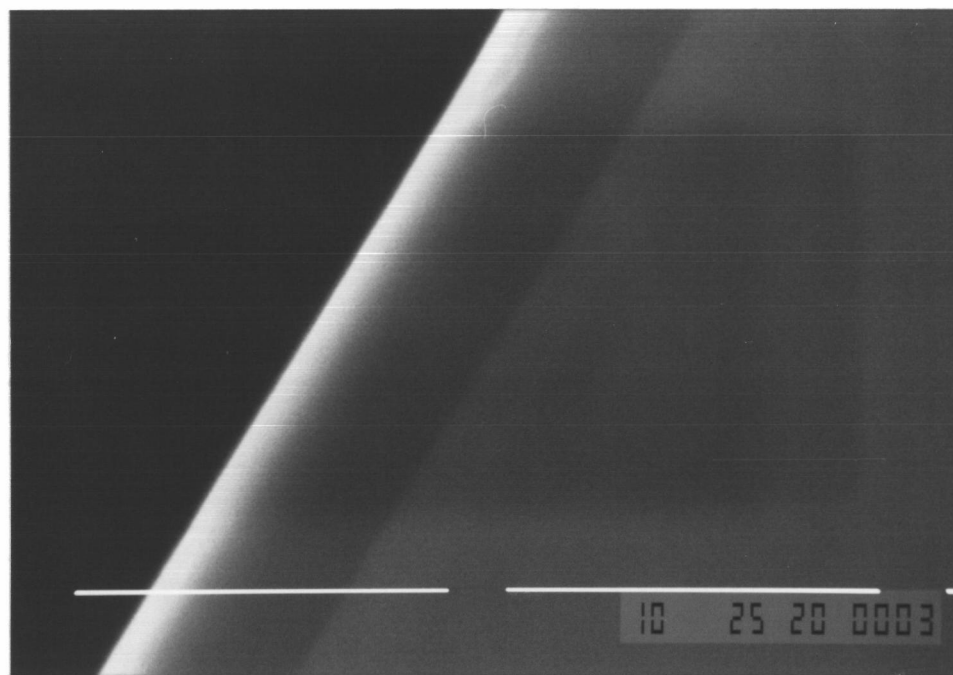


Figure 4.2 The SEM image of the MBE growth  $\text{Al}_{0.58}\text{Ga}_{0.42}\text{As}$  and GaAs layers on the GaAs substrate used for preparing shadow mask.

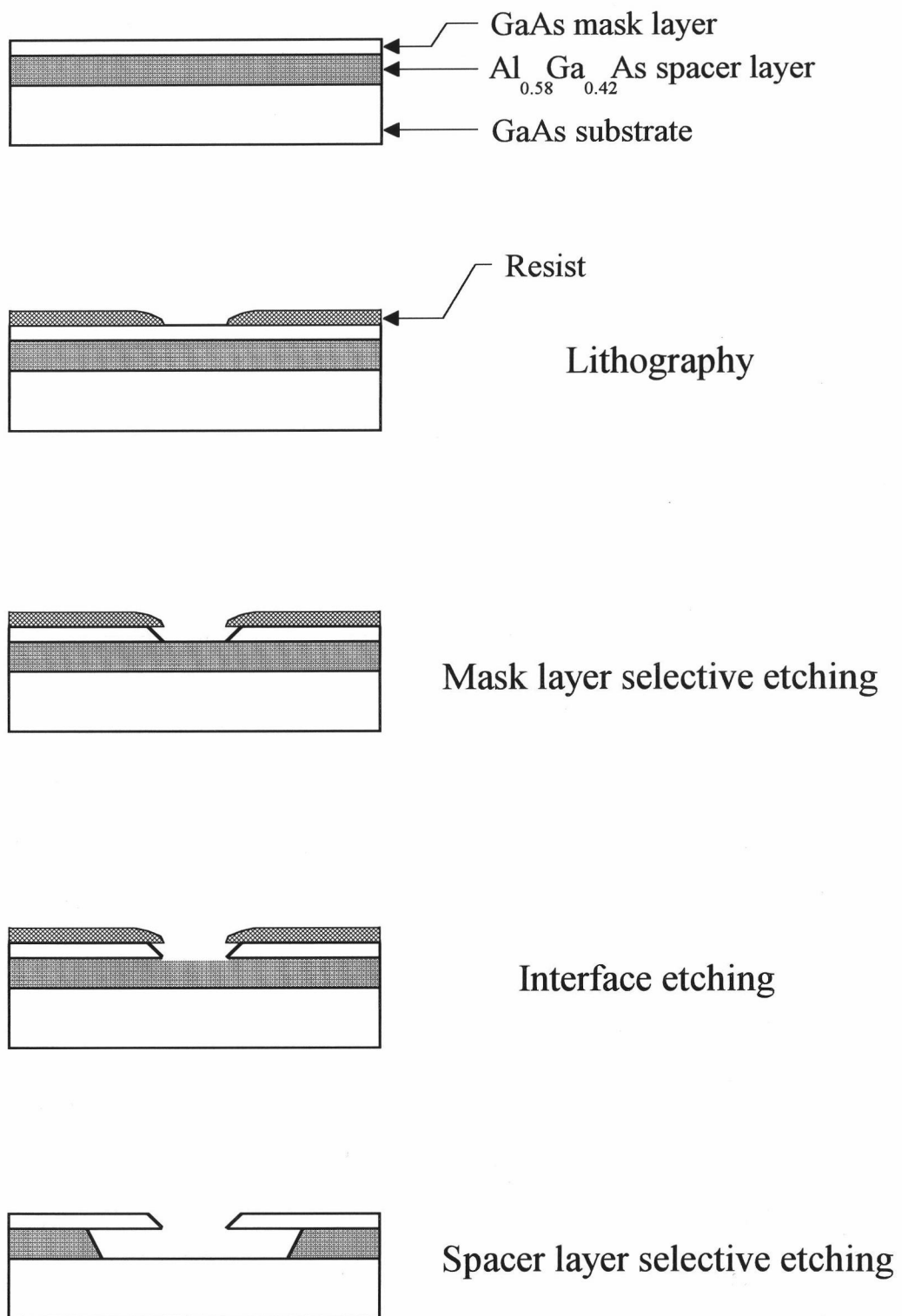


Figure 4.3 Shadow mask preparing process diagram.

A shadow mask preparing process is illustrated in figure 4.3. The wet chemical etching was used in the subprocesses. The mask layer was patterned using conventional lithography and etched with solution of  $\text{H}_3\text{PO}_4 : \text{H}_2\text{O}_2 : \text{H}_2\text{O} = 1 : 1 : 10$  (by volume) for 80 seconds to open the windows on the mask layer. This solution is anisotropic-selective etchant that can etch GaAs in direction  $\langle 100 \rangle$  much faster than direction  $\langle 111 \rangle$  and stop at  $\text{Al}_x\text{Ga}_{1-x}\text{As}$  interface. The edges of the patternized windows then form as wedge-shape as shown in figure 4.4. Line shaped window patterns of  $7 \mu\text{m}$  and  $5 \mu\text{m}$  width and  $250 \mu\text{m}$  separations were provided for the experiment. The  $\text{Al}_{0.58}\text{Ga}_{0.42}\text{As}$  mask spacer under the pattern can be removed by using  $\text{KI} : \text{I}_2 : \text{H}_2\text{O} = 12 \text{ g} : 3 \text{ g} : 10 \text{ ml}$ . This solution is AlGaAs selective etchant which etch-rate is higher than 40:1 for the Al content  $> 50\%$ . By this nature, to ensure the successfully subsequence etching of the mask spacer, the GaAs and  $\text{Al}_{0.58}\text{Ga}_{0.42}\text{As}$  interface should be etched with solution of  $\text{NH}_4 : \text{H}_2\text{O}_2 : \text{H}_2\text{O} = 3 : 1 : 15$  (by volume) for 15 seconds. The interface etching solution can etch either GaAs or any Al content of AlGaAs and forming the facet along the  $\langle 1\bar{1}0 \rangle$  direction.

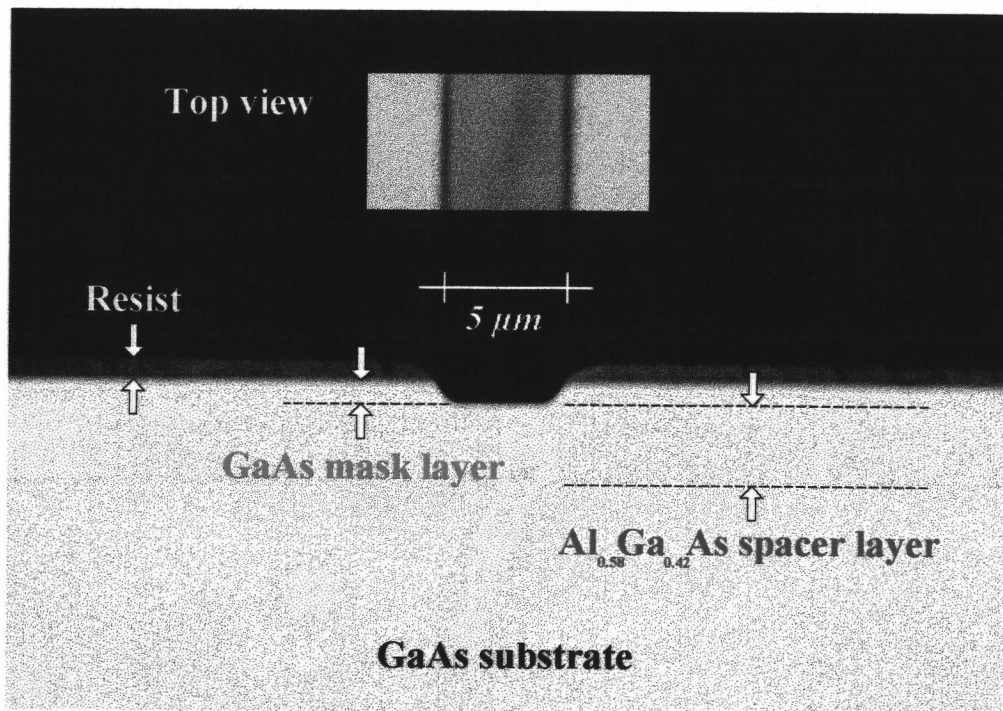


Figure 4.4 Optical microscope cross sectional view after mask layer etching process.



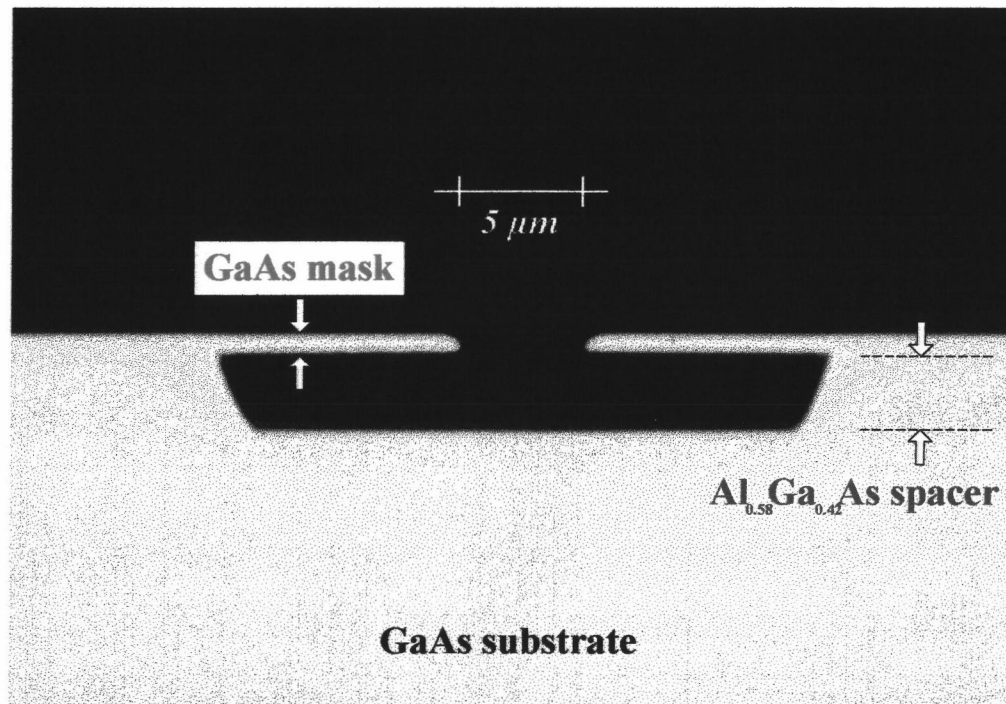


Figure 4.5 Optical microscope cross sectional view after spacer layer etching process.

After removal of the remaining photoresist using hot acetone and rinsed with DI-water then the mask spacer was etched using the solution that described before. This step of the remaining resist removal before the spacer etching is very important. The surface that needed to selective growth should be free from contamination. If the resist was removed in the last step, capillary effect by the small patterns could disobey the dissolved resist. Then it remains in the shadow mask and causes contamination. An etching time for the mask spacer is controlled by factor of the layer thickness and requirement of the cantilever mask layer length. For the 3 μm thickness, the etching time is 1 minute then providing cantilever length of 10 μm. The optical micrograph cross-sectional view of shadow mask is shown in figure 4.5. Then, the very smooth surface in the bottom of the mask window is appeared and ready to go into the epitaxial regrowth process.

## 4.2 Growth of Multiple Quantum Well through Shadow Mask

There were 3 samples fabricated in this experiment.

Sample #1 : This is a reference sample from the previous chapter of MQW growth. The MQW structure was grown on the plain (100) GaAs substrate.

Sample #2 : The sample that was prepared with 7  $\mu\text{m}$  wide line patterns.

Sample #3 : The sample that was prepared with 5  $\mu\text{m}$  wide line patterns.

A conventional MBE method was used to fabricate series of GaAs/ $\text{Al}_{0.2}\text{Ga}_{0.8}\text{As}$  to form structure of 10 identical unit quantum wells. There are two different well widths, 60 monolayers and 30 monolayers. The sample #1 and sample #3 have 60 monolayers well width and the sample #2 has 30 monolayers well width. The barrier thickness of all samples is 300 monolayers. Clean surface of GaAs mask layers and GaAs substrate under shadow masks is confirmed by RHEED pattern before each MBE growth. Substrate temperature during the growths was 650 °C while the substrates were rotated at 4 rpm for uniformity. Al and Ga molecular beam flux were  $2 \times 10^{-7}$  Torr and  $2.5 \times 10^{-7}$  Torr, respectively, while  $\text{As}_4$  molecular beam flux was  $1.5 \times 10^{-5}$  Torr for all samples. With these conditions, growth rate was resulted around 1 monolayer (ML) per second in conventional MBE growth.

Figure 4.6 and 4.7 show the cross sectional views of shadow masked mesa MQW by an optical microscope and a scanning electron microscope (SEM), respectively.

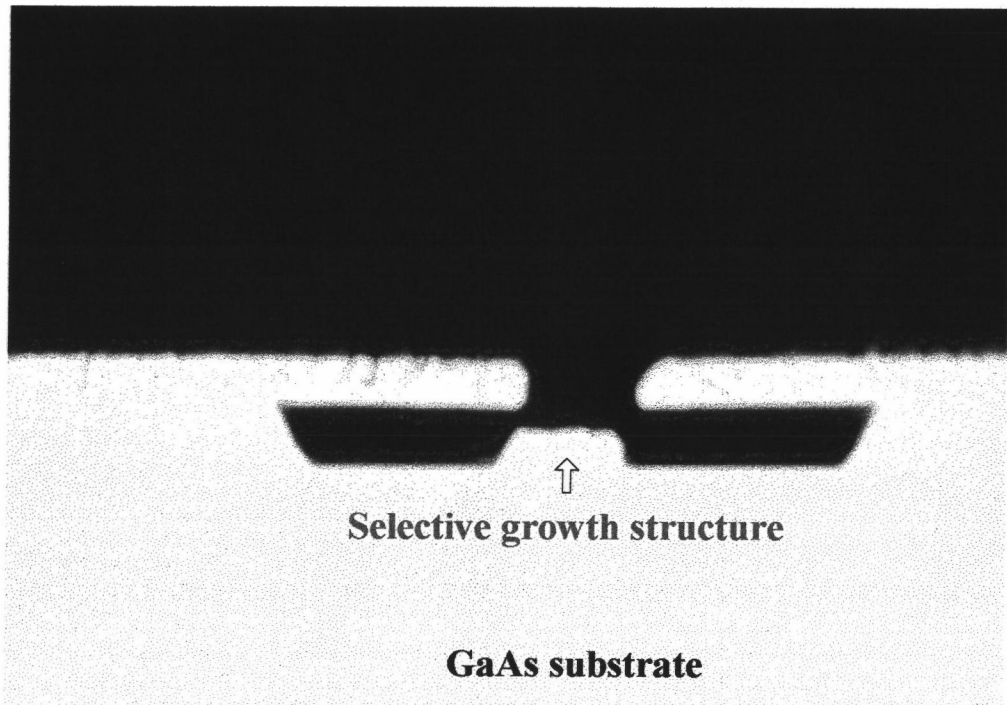


Figure 4.6 Optical microscope cross sectional view of the sample #3 after 10MQW structure grown.

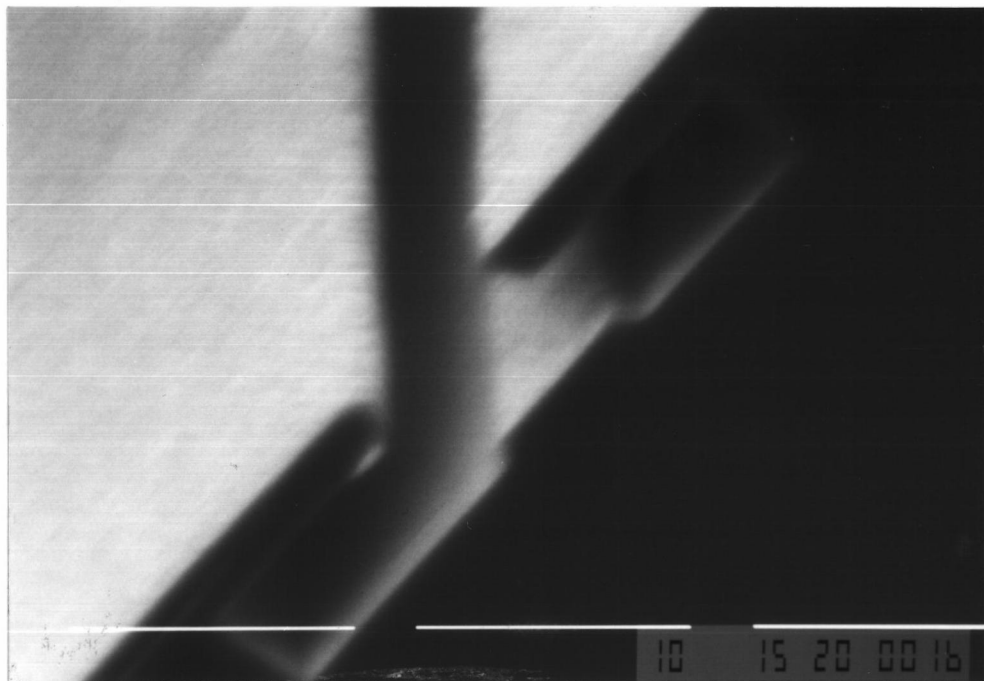


Figure 4.7 SEM micrograph of the sample #2.

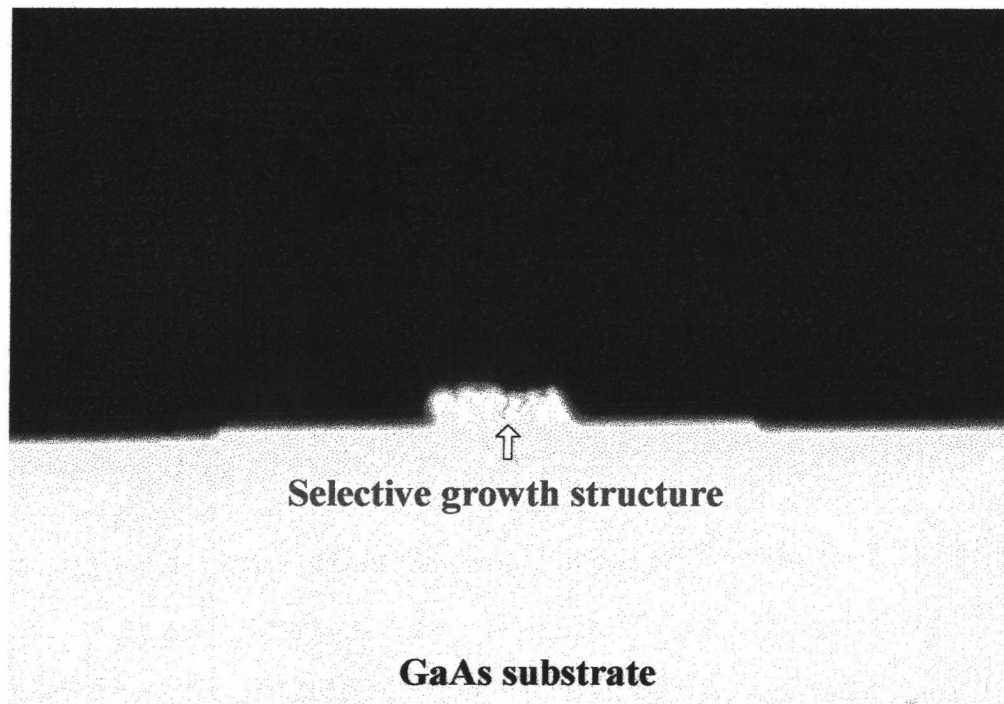


Figure 4.8 Optical microscope cross sectional view of the sample #3 after strip-off process.

Furthermore, after MBE growth process, a part of sample #3 was passed through a strip-off procedure by second reverse photolithography. The mesa-line structures were protected by photoresist after the photolithography process. Shadow masks and GaAs/ $\text{Al}_{0.2}\text{Ga}_{0.8}\text{As}$  quantum well structures grown over the masks were then partially removed with  $\text{NH}_4\text{OH} : \text{H}_2\text{O}_2 : \text{H}_2\text{O} = 3 : 1 : 15$  (by volume). Figure 4.8 shows a cross sectional view of mesa-MQW after the strip-off to eliminate the shadow masks for effectiveness of MQW signal.

### 4.3 Photoluminescence Results

The photoluminescence (PL) measurements were conducted by using 50 mW Ar<sup>+</sup> laser as the excitation of all samples set up in 10 K cryogenic system. The laser beam was point focused by a circular lens and was line focused by a cylindrical lens onto the stripes of MQW. The line focus could be aligned parallel to the stripes (0°) and perpendicular to the stripes (90°) for analysis of the PL results. The focusing dimension was ~100 μm for spot and line.

Figure 4.9 shows PL spectra of shadow masked mesa-MQW stripes with 7 μm wide (Sample #2) when the sample was excited by point and line of laser beams both at 0° and 90° configurations. Multi-peak photoluminescence spectrum have been observed. To simplify the position of each peak, the dash lines in the figures were created by using *Multiple Gauss fitting* utility in Origin™ plotting program.

Double PL peaks at 758 and 774 nm were observed in all cases. The strongest PL peaks were obtained by point focus due to the most intense excitation laser beam. In case of line focus, at parallel configuration, the sample gave nearly equal intensity of double PL peaks but less strong signals due to shadow mask effect in optical alignment of PL experimental set. At 0° configuration, PL peaks become weaker due to the smaller effective area. The separation of these double PL peaks (about 16 nm) could be explained by the variation of narrow quantum well widths between MQW on shadow mask and mesa MQW underneath. The quantized states of electrons in quantum wells are changed.

Figure 4.10 shows PL results from sample #3. An objective for preparing this sample is to provide a tunability of the quantized state in the shadow masked MQW. Overlapping of PL peaks at 810 nm came from MQW structure that was fabricated onto the mask layer and at 818 nm came from the MQW structure that was grown through the shadow mask were observed and the peak position referred to the previous experiment.

The strongest PL peaks were again observed by point focus due to the most intense excitation of laser beam. However, line focus at 0° configuration gave lowest PL peaks due to narrower window and this made PL alignment more difficult. When the sample was rotated to 90° configuration, PL alignment becomes easier and better PL signals were detected.

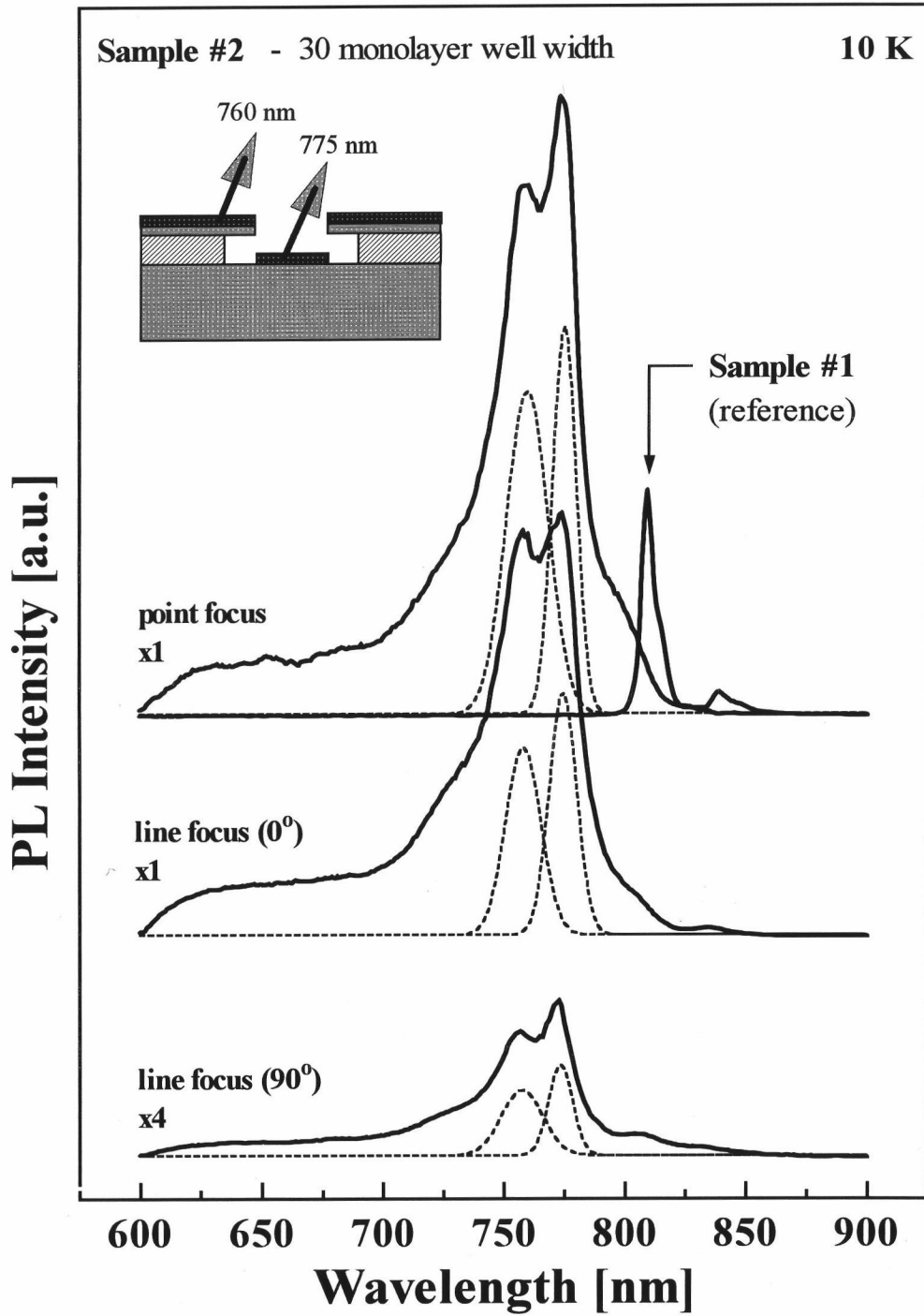


Figure 4.9 Comparison of the PL spectrum from sample #1 as a reference and sample #2.

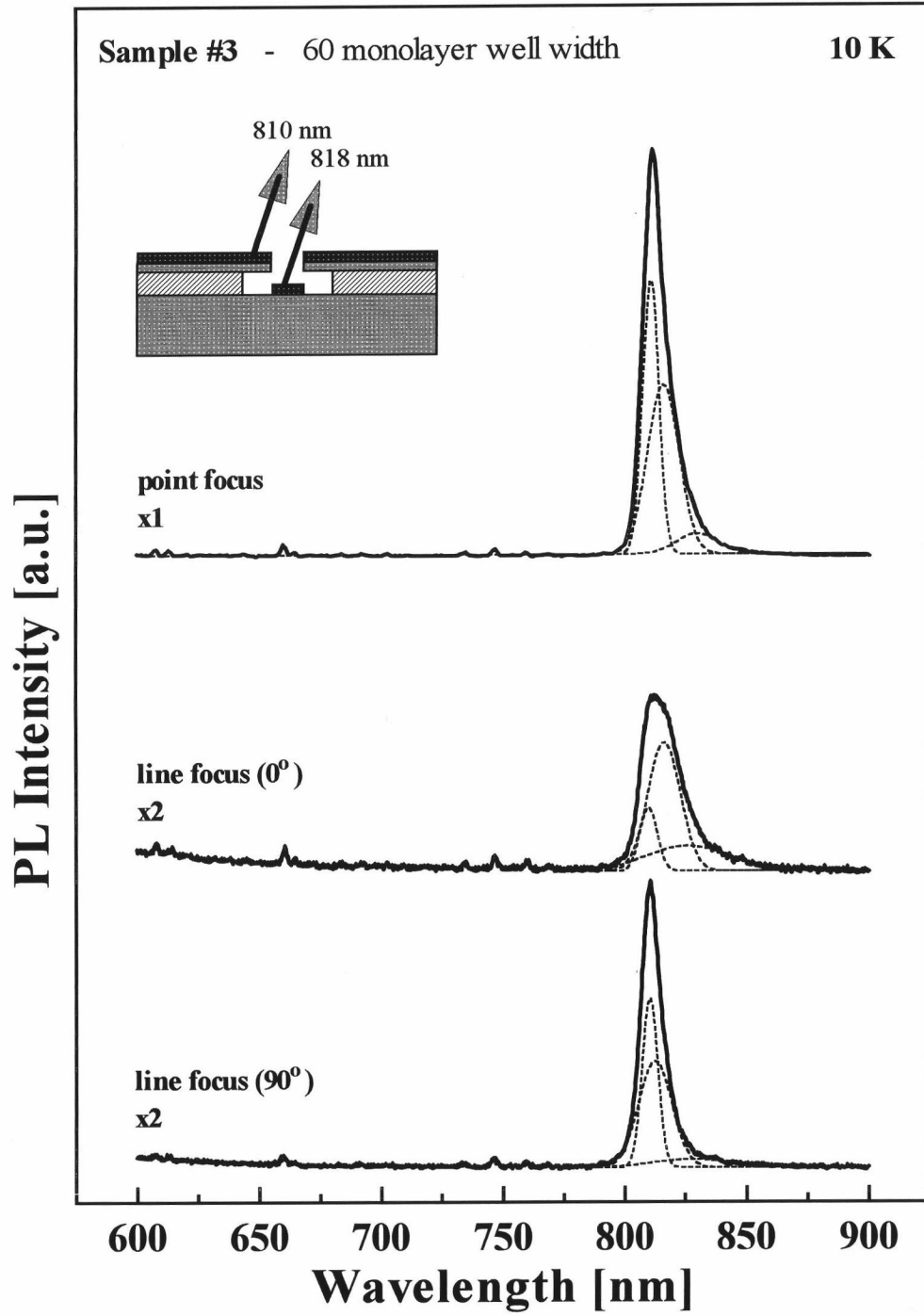


Figure 4.10 The PL spectrum from sample #3.

The variations of the peak position came from shadow masking effect that causes  $As_4$  flux was reduced in the small volume under the shadow mask. The growth rate of the mesa under the shadow mask has been changed. The  $As_4$  flux stability under the shadow mask affects to the undulated surface on shadow masked mesa. During the growth of MQW structures, Ga islands are formed due to less of  $As_4$  flux. This 3D growing seems to be related to the broadening of the PL signal [6]. PL peaks from the shadow masked mesas in all samples have shown some broader than the peaks from the MQW over the masks.

To ease the PL alignment, shadow masks of sample #3 were partially strip-off and were experimented under the same conditions. The only strongest PL peak was always at 818 nm that corresponded to the mesa-MQW stripe while the PL peak at 810 nm was comparatively much smaller. The best configuration for strip-off sample was line focus at  $0^\circ$  position due to efficient PL alignment that becomes more effective than point focus excitation. The line focus at  $90^\circ$  configuration still gave weak PL peaks, but PL signals from strip-off sample were always stronger than those from shadow masked samples as shown in figure 4.11. PL peaks were about 3 times stronger after the strip-off process.

All PL spectra from both sample #2 and #3 have nearly the same full width at half maximum (FWHM) from 14-16 nm that are broad comparing with 5 nm that obtained from the reference PL peaks from plain surface MQW sample (Sample #1) due to un-optimization growth conditions as described. However, PL spectrum from the MQW shadow masked mesas show a possibility and advantage of the shadow mask technique for growing *in-grown* patternized epitaxy by MBE.



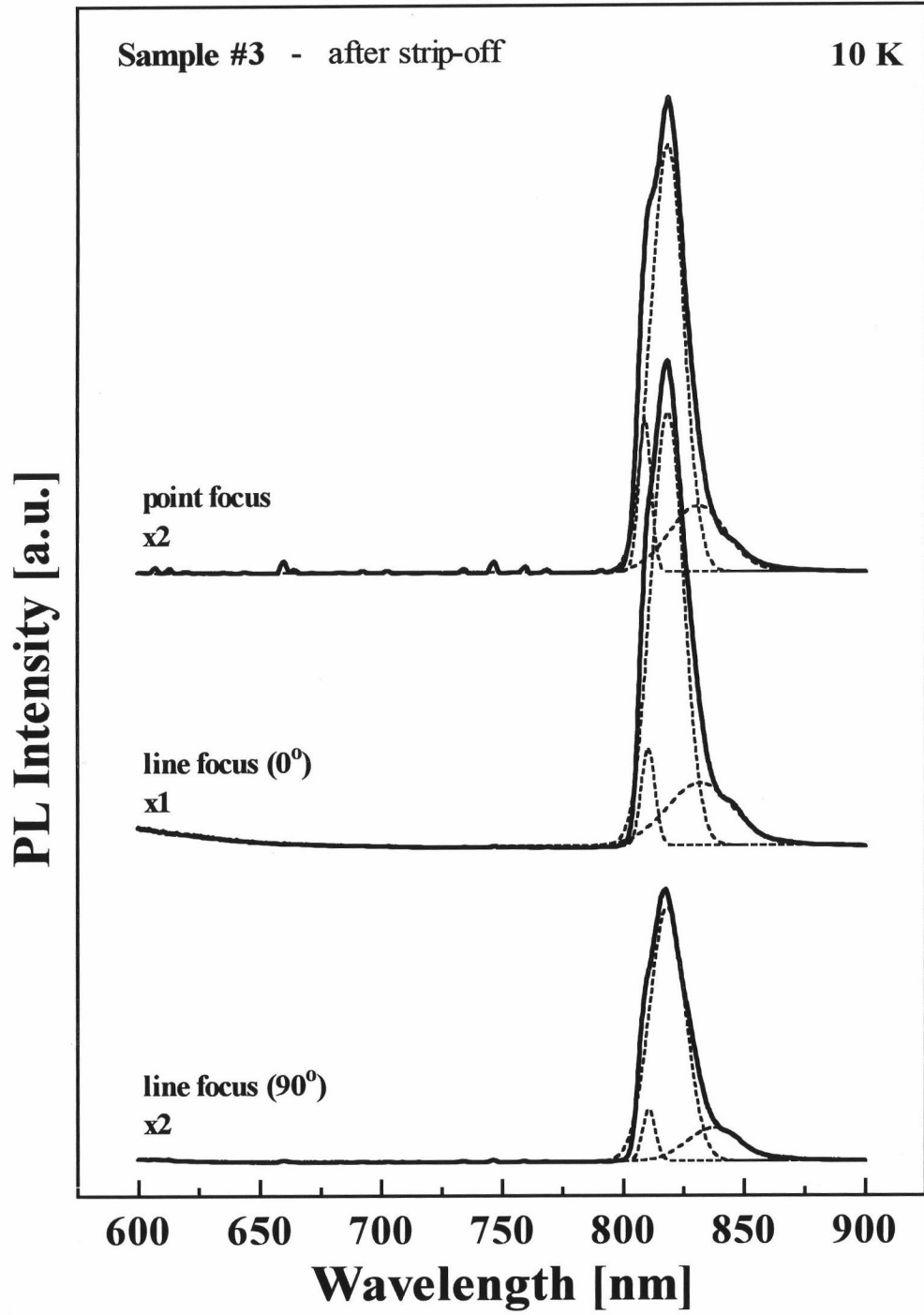


Figure 4.11 The PL spectrum from sample #3 after strip-off process.

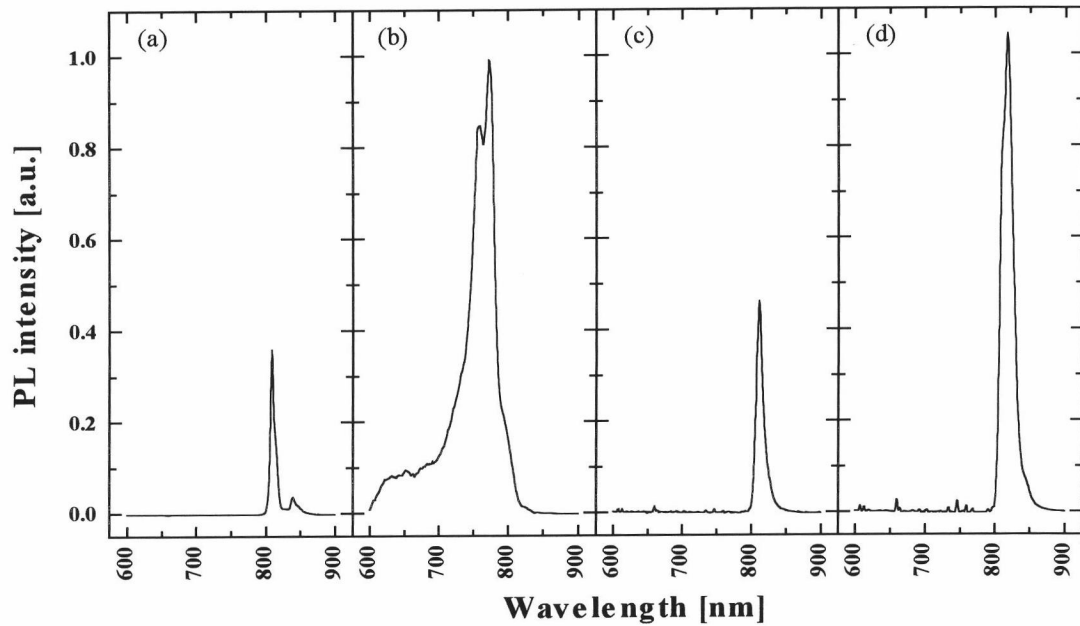


Figure 4.12 The comparison of all samples with same scaling

- (a) Sample #1 : plain 60 ML quantum well width, as the reference
- (b) Sample #2 : Shadow mask 7  $\mu\text{m}$  width, 30 ML quantum well width
- (c) Sample #3 : Shadow mask 5  $\mu\text{m}$  width, 60 ML quantum well width
- (d) Sample #3 : After the strip-off process

Figure 4.12 compares the point-focused PL spectrum reviewing in the same axis scaling. The spectrum (b) and (d) seem to have same intensity, but the spectrum from sample #2 is strong although the mask was not stripped off. Wider window of the mask lets the PL signal spreading out more than from narrower stripe window having small amplitude as shown by spectrum (c). An important point is that the shadow masked mesas give stronger PL intensity than that from the plain MQW epitaxy by factor more than 2.85 in any event from 7 or 5  $\mu\text{m}$  stripe width. It is confirmed that shadow mask is a preferable growing technique by which can fabricate excellent mesa structures without any etched mesa sidewalls.

From a problem of the undulation morphology of the shadow masked mesas due to the estimation of  $\text{As}_4$  flux stabilization during MBE growth, a new shadow mask sample was prepared. 3  $\mu\text{m}$  stripe patterns are generated. During the MBE growth,  $\text{As}_4$  flux intensity was increased to  $2.5 \times 10^{-5}$  Torr. while other cells remained the same as the growth processes before. Figure 4.13 and 4.14 are cross-sectional and perspective view SEM micrographs of this sample. The morphology of this sample was significantly improved.

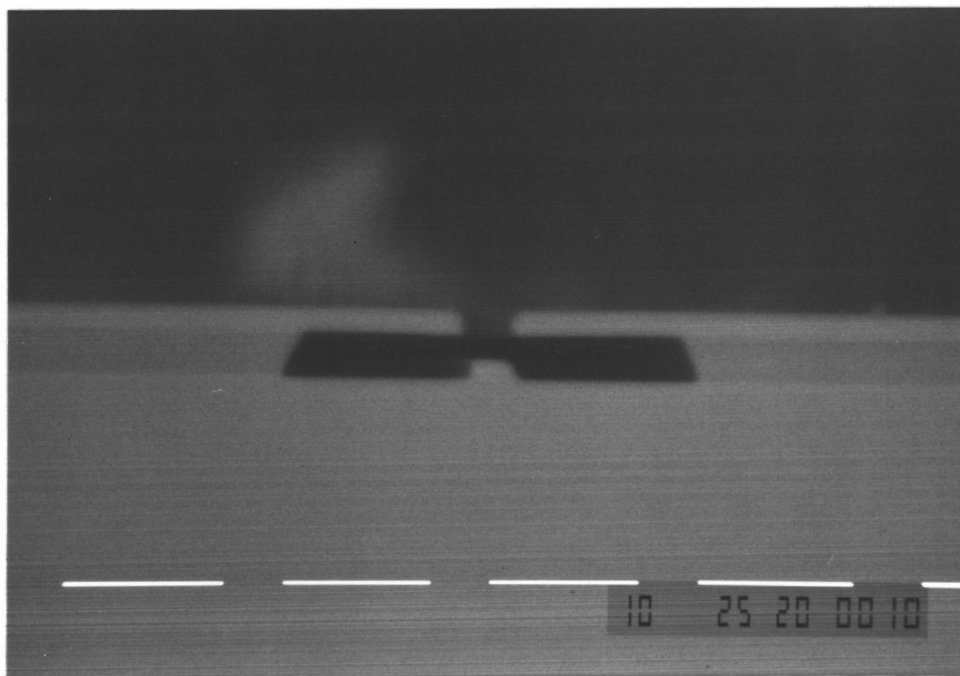


Figure 4.13 Cross-sectional view SEM of the shadow mask after MBE growth with  $\text{As}_4$  increasing.

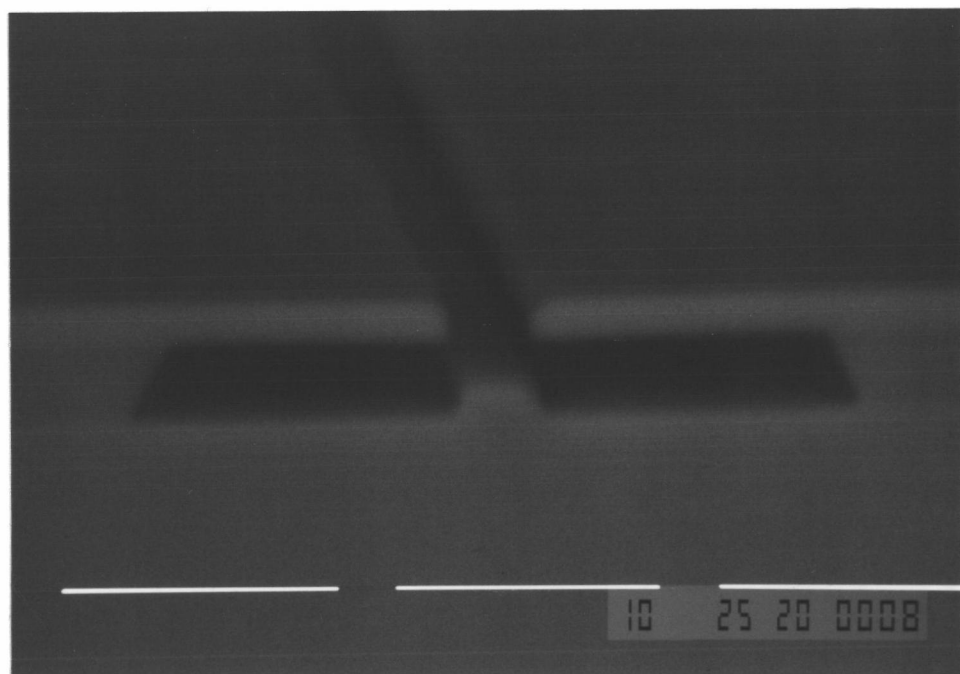


Figure 4.14 Perspective view SEM micrograph, surface morphology of the shadow masked mesa was relatively improved.